Internal Energy Distributions of OH Products in the Reaction of O(^3P_J) with HSiCl$_3$

Hyon Tae Kwak, Seung Chul Ha,* Sungwoo Jang, Hong Lae Kim,‡ and Chan Ryang Park*

*Department of Chemistry, Kookmin University, Seoul 136-702, Korea. *E-mail: crpark@kookmin.ac.kr*
**Kolmar Korea Co., Yunki-gun, 170-7, Chungnam 339-851, Korea*
‡Department of Chemistry and Institute of Molecular Science and Fusion Technology, Kangwon National University, Chuncheon 200-701, Korea
Received December 31, 2008, Accepted January 3, 2009

The OH($X^2\Pi$, v''=0, 1) internal state distributions from the reaction of electronically ground state oxygen atoms with $HSiCl_3$ were measured using laser-induced fluorescence. The ground-state O(^3P_J) atoms with kinetic energies above the reaction barrier were produced by photolysis of NO_2 at 355 nm. The OH product revealed strong vibrational population inversion, $P(v''=1)/P(v''=0) = 4.0 \pm 0.6$, and rotational distributions in both vibrational states exhibit substantial rotational excitations to the limit of total available energy. However, no preferential populations in either of the two Λ doublet states were observed from the micropopulations, which supports a mechanism involving a direct abstraction of hydrogen by the atomic oxygen. It was also found that the collision energy between O and $HSiCl_3$ is effectively coupled into the excitation of the internal degrees of freedom of the OH product ($\langle f_{vib}\rangle = 0.62$, and $\langle f_{rot}\rangle = 0.20$). The dynamics appear consistent with expectations for the kinematically constrained reaction which supports the reaction type, heavy + light-heavy → heavy-light + heavy (H + LH′ → HL + H′). The dynamics of oxygen atom collision with $HSiCl_3$ are discussed in comparison to those with SiH_4.

Key Words: Trichlorosilane, O(^3P_J), LIF, OH, Internal energy distribution

Introduction

The reaction of atomic oxygen with a variety of hydrogen-containing compounds still attracts many attentions up to now. Both theoretical and experimental investigations on oxygen atom reactions with various types of new substrates[1] have been conducted recently. The reactivity of atomic oxygen plays an important role in establishing the chemistry of such processes as combustion and semiconductor processes.[2] While the kinetic studies[3] of elementary reactions involving O(^3P_J) have been numerous, the studies of their dynamics[4] are relatively sparse. One of the earliest experimental investigations was focused on the typical reaction of O(^3P_J) with saturated hydrocarbons,[5] i.e., methane, ethane, propane, *iso*-butane and, etc.

$$O(^3P_J) + RH \rightarrow OH(X^2\Pi) + R \qquad (1)$$

The energetics of the OH($X^2\Pi$) product from reaction 1 were characterized by laser-induced fluorescence (LIF). Where permitted by the reaction exothermicity, vibrational excitation of the diatomic results: an observation consistent with a mechanism in which O(^3P_J) directly abstracts a hydrogen atom from the hydrocarbon substrate.

The reaction of O(^3P_J) with silane compounds, typified by the reaction 2, also resulted in a substantial inversion of the OH vibrational population distribution, with values of $P(v''=1)/P(v''=0) = 3.4 \pm 0.4$.[6]

$$O(^3P_J) + SiH_4 \rightarrow OH(X^2\Pi) + SiH_3 \qquad (2)$$

The rotation of the OH($X^2\Pi$, v''=1) product resulting from reaction 2 showed complete thermal distributions with T_{rot} = 600 ± 20 K. That of the OH($X^2\Pi$, v'' = 0), however, displays a thermal distribution (T_{rot} = 750 K) only below N'' = 6. At higher N'' states to the limit of available energy, the distribution inverts in a manner similar to that observed in OH resulting from the reaction of O($^1D_2$) with some hydrocarbons.[7] Both the strong vibrational population inversion and the thermal rotational distributions could be interpreted in terms of a simple abstraction mechanism. The observation of anomalously high populations in the rotationally excited states of OH in its ground vibrational state has led to the suggestion of a possible presence of a reaction intermediate: a pentacoordinate silicon-centered collision complex.[5,6]

A recent study[8] of the reaction 3 also revealed a substantial rotational excitation extending to the limit of available reaction exoergicity at each vibrational level, along with the strong vibrational population inversion ($P(v''=0)$: $P(v''=1)$: $P(v''=2)$ = 0:9:1).

$$O(^3P_J) + HBr \rightarrow OH(X^2\Pi) + Br \qquad (3)$$

This rotational excitation of OH was rationalized by consideration of the different angular dependence of model potential surfaces which satisfactorily reproduced the observed dynamics. This study accented the importance of the curvature of the potential hypersurface orthogonal to the reaction coordinate in establishing the degree of rotational excitation in the products, which was interpreted as signifying a low barrier to bending in the O-H-Br transition state. More recently, the rotational, spin-orbit, and Λ doublet populations of the OH(v''= 1) product from the reaction of O(^3P_J) with H_2S have also been reported,[9] and the rotational distributions of

OH(υ"= 1) were found to be hotter than statistically predicted ones with excitation up to the energetic limit.

To test the role played by collision complex barriers to rotational excitation, the rotational distribution of OH product following the reaction 4 was examined using the LIF method assuming no dramatic difference between the O/SiH_4 and the $O/(CH_3)_3SiH$ potentials along the reaction coordinate.[10]

$$O(^3P_J) + (CH_3)_3SiH \rightarrow OH(X^2\Pi) + (CH_3)_3Si \quad (4)$$

The presence of three methyl groups on $(CH_3)_3SiH$ obviously constrains the bending of the collision complex about the hydrogen atom (O-H-Si) and hence limits the amount of rotational excitation in the diatomic product. As expected, the rotational distributions of $OH(X^2\Pi)$ in both accessible vibrational states turned out to be very cold and well characterized by Boltzmann temperatures, $T_{rot}(\upsilon"=0) = 770 \pm 20$ K and T_{rot} $(\upsilon"=1) = 173 \pm 10$ K. The reactions of atomic oxygen with silane and trimethylsilane provide a good illustration of the role played by transition-state dynamics in establishing energy deposition in elementary reactions.

The present experiments probe the dynamics of the reaction.

$$O(^3P_J) + HSiCl_3 \rightarrow OH(X^2\Pi) + SiCl_3 \quad (5)$$

a process that is interesting from a view point of a reaction kinematics compared with that of reaction 2. Since the bond dissociation energy of $HSiCl_3$ (D_0(H-Si) = 91.30 kcal/mol)[11] is slightly larger than that of SiH_4 (D_0(H-Si) = 90.34 kcal/mol),[12] the exothermicity of the reaction 5 is lower than that of the reaction 2. On the other hand, because the $HSiCl_3$ is heavier than SiH_4, more of the excess O-atom translational energy arising from the NO_2 photolysis appears in the center-of-mass frame of the collision in reaction 5. As a result, the total available energies for both reactions 2 and 5 are estimated about the same. Moreover, since both reactions consist of the 'an atom + five-atom-molecule' system, the number of total degrees of freedom is the same for both reactants and products. Hence the effect of the collision energy on partitioning of the available energy into the internal modes of the products is expected to be easily compared with relatively little ambiguity.

Experiments

The procedures followed in the present experiment were essentially identical with a typical photolysis-probe LIF experiment using a flow cell. In brief, the $OH(X^2\Pi)$ products following reaction 5 were monitored shortly after the initial formation of $O(^3P_J)$ in the UV laser photodissociation of NO_2. Observation of the nascent OH population distributions was ensured by minimizing both the delay time (< 200 ns) between the photolysis and excitation lasers, and the ambient gas pressure (< 200 mtorr) in a reaction cell.

It is well known that photodissociation of NO_2 below the threshold wavelength for predissociation yields the ground state atomic oxygen

$$NO_2 + h\nu\ (\lambda < 400\ nm) \rightarrow NO + O(^3P_J) \quad (6)$$

In the present work, 355-nm photolysis of NO_2 is accomplished with the 3rd harmonic of Nd:YAG laser(Spectra Physics, DCR-11). Less than 10% of the NO_2 in the reaction zone was estimated to decompose with each laser pulse (E_{laser} = *ca.* 100 mJ cm^{-2}, repetition rate = 10 Hz). Photodissociation of NO_2 above the energetic threshold results in the production of translationally excited $O(^3P_J)$. Molecular beam studies[13] of reaction 6 reveal roughly equal populations of NO in υ"=0 and 1 following photolysis at 347.1 nm. Assuming similar behavior following photodissociation at 355 nm, we calculated a collision energy of *ca.* 1,440 cm^{-1} in the center of mass frame of $O/HSiCl_3$.

Approximately 100 ns following the initiating laser pulse, another Nd:YAG laser-pumped(2nd harmonic, 532 nm, Spectra Physics GCR-150), frequency-doubled, tunable dye laser (Lumonics HD500, $\Delta\lambda$ = 0.002 nm) probes the population of $OH(X^2\Pi, \upsilon", N", f", \lambda")$ by exciting the (0,0) and (1,1) bands of the $A^2\Sigma - X^2\Pi$ transition in the range 306-318 nm. The unresolved total fluorescence is subsequently collected at right angles to the counterpropagating photolysis and probe laser beams with a high-gain photomultiplier tube (Hamamatsu, R2059) viewing through a broad-band ultraviolet filter consisting of UG-11 glass and 10 cm of 1 M $NiSO_4$ solution. This filter combination is very efficient in attenuating the scattered photolysis light at 355 nm. The electronic signal from the PMT is then sampled with a boxcar (EG&G 4161A, 4121B) and recorded in a laboratory computer system. All the equipments are controlled and synchronized *via* LabVIEW program.

Conversion of the measured LIF signal S to state-resolved $OH(X^2\Pi)$ population requires correction for variation in the intensities of both the photolysis and probe lasers, I_{photo} and I_{probe}, as well as accurate values of the Einstein coefficients, $B_{\upsilon"J"}^{\upsilon'J'}$, for stimulated emission. Laser intensities were monitored and recorded simultaneously with the LIF signal during spectral scans. Tabulated values of $B_{\upsilon"J"}^{\upsilon'J'}$ provided by Crosley are used throughout.[14]

$$P(\upsilon", N", f", \lambda") \propto \frac{S}{I_{photo} \cdot I_{probe} \cdot B_{\upsilon"J"}^{\upsilon'J'}} \quad (7)$$

Electronic quenching of $OH(A^2\Sigma)$ by ambient gases is assumed negligible[15,16] under the given experimental conditions. The populations derived from Eq. 7 need not be corrected for predissociation of the excited state because the highest rotational levels formed are well below the crossing of the $^4\Sigma^-$ state near 5,300 cm^{-1} of $A^2\Sigma$.[17] The linearity of the LIF measurements was confirmed by comparing the relative intensities of satellite and main branch transitions that probe the same level of $OH(X^2\Pi, \upsilon", N", f", \lambda")$.

Nitrogen dioxide (NO_2, 99.5%, MG Industries) and trichlorosilane ($HSiCl_3$, 99%, Aldrich) were purified of low-boiling impurities by multiple freeze-thaw cycles. Especially, for further purification of NO_2, excess pure O_2 was added and pumped out to remove NO impurities which might be present in the sample. The experiments were carried out at a total

Table 1. Observed OH Population Distributions following the Reaction of O(^3P_J) with SiH_4 and $HSiCl_3$

	$P(A')/P(A'')$		$P(^2\Pi_{3/2})/P(^2\Pi_{1/2})$		Rotation		$P(\upsilon''=1)/P(\upsilon''=0)$	Ref.
	$\upsilon''=0$	$\upsilon''=1$	$\upsilon''=0$	$\upsilon''=1$	$\upsilon''=0$	$\upsilon''=1$		
O + SiH_4	1.28 ± 0.1	1.0 ± 0.1	1.22 ± 0.1	1.5 ± 0.2	inverted	thermal	3.4 ± 0.4	6
O + $HSiCl_3$	1.07 ± 0.1	0.90 ± 0.1	1.06 ± 0.1	1.13 ± 0.1	inverted	inverted	4.0 ± 0.6	This work

Table 2. II: Disposal of Energy into Internal Modes of Product OH

	$-\Delta H^0$/cm^{-1}	$\langle E_{coll}\rangle$/cm^{-1}	$\langle E_{avail}\rangle$/cm^{-1}	$\langle f_{rot}(OH)\rangle^a$	$\langle f_{vib}(OH)\rangle^a$	Ref.
O + SiH_4	3,500	1,110	4,610	0.15	0.60	6
O + $HSiCl_3$	3,150	1,440	4,590	0.20	0.62	This work

$^a\langle f_{rot}(OH)\rangle = \langle E_{rot}\rangle/\langle E_{avail}\rangle$, $\langle f_{vib}(OH)\rangle = \langle E_{vib}\rangle/\langle E_{avail}\rangle$

pressure of 160 mTorr in a 50:50 mixture in the flow cell. Both reagents were prepared in a standard mercury- and grease-free glass vacuum line, and a precaution was taken to mix the reactants right before the reaction zone to minimize a possible pre-reaction of NO_2 with $HSiCl_3$.

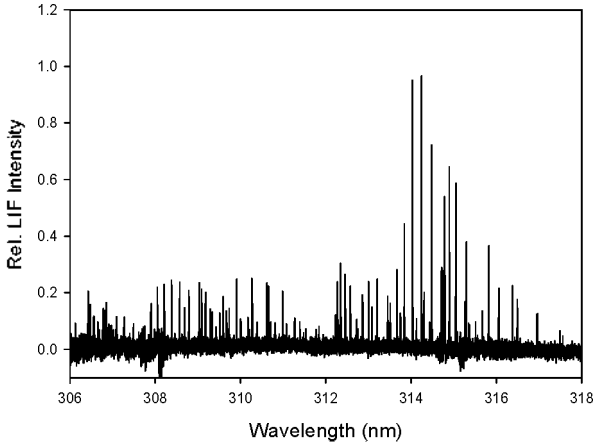

Figure 1. Merged LIF spectrum of the OH product arising from O(^3P_J) + $HSiCl_3$ → OH($X^2\Pi$) + $SiCl_3$ obtained under the experimental conditions described in the text. The signal intensities have been corrected for variations of I_{photo} and I_{probe}.

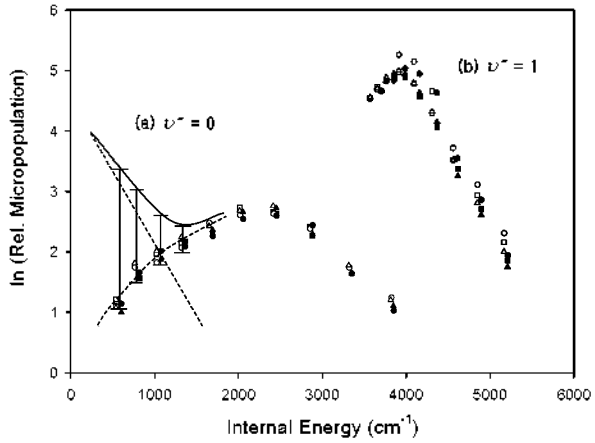

Figure 2. Micropopulation distributions of the OH products derived from experimental spectrum: (a) $\upsilon''=0$; (b) $\upsilon''=1$. These were obtained from the following transitions: P_{11}(□), P_{22} (■), Q_{11} (○), Q_{22}(●), R_{11}(△), R_{22}(▲). The micropopulations of OH($N''\leq 6$ in $\upsilon''=0$) are corrected to account for the contribution of OH produced from direct photodissociation of HONO. The upper bounds of the errors are presented. (see text)

Results and Discussion

LIF Spectrum and Micropopulations. The LIF spectrum observed following reaction 5 (Figure 1) displays the characteristic OH($A^2\Sigma^- \leftarrow X^2\Pi$) transitions[18] corresponding to absorption by diatomic molecules formed in $\upsilon''=0$ and 1. Extensive population of OH($X^2\Pi$, $\upsilon''=1$) can clearly be discerned; the R-band head of (1,1) band begins at *ca.* 312 nm and that of (0,0) band at *ca.* 306 nm. Conversion of the spectrum to micropopulations (the state populations divided by their rotational degeneracy, $2J''+1$) yields the distributions displayed in Figure 2; it is plotted in log scale so that the slope of the distribution represents a Boltzmann type rotational temperature. Substantially inverted vibrational and rotational populations are apparent at a glance.

It has been reported by previous studies[8,9,19] that photolysis of NO_2 as an O(^3P) atom source causes a problem because of the fact that photolysis of HONO formed from NO and H_2O impurities *via* reaction 8 also produces OH.

$$NO_2 + NO + H_2O \rightleftharpoons 2HONO \qquad (8)$$

The 355 nm photolysis of HONO produces vibrationally and rotationally cold OH($X^2\Pi$), predominantly in the $\upsilon''=0$,

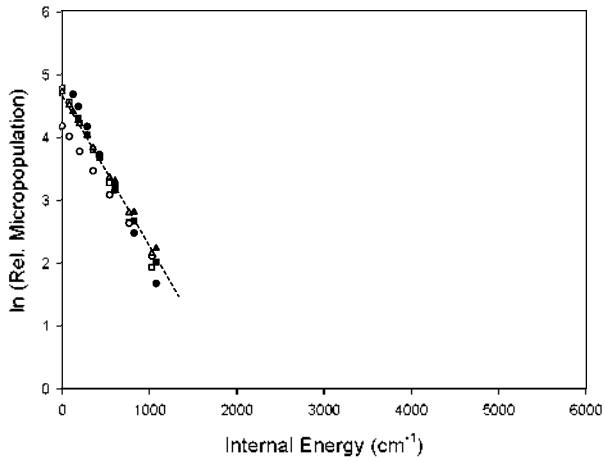

Figure 3. Micropopulation distributions of the OH($\upsilon''=0$) products produced from reaction 8. The same data-labeling convention is used as in Figure 2. The fitting line represents a thermalized rotational temperature of T_{rot} = 560 K.

$N'' \leq 6$ states and no OH product was found in $v''=1$ state from the photolysis of NO_2 alone. In our experiment, since the HONO contribution to the OH signal in $v''=0$ could not be eliminated completely, the OH($v''=0$) rotational population obtained from photolysis of NO_2 alone was subtracted from that obtained from reaction 5 assuming a linear rotational surprisal[20] in the $N'' \leq 6$ states.

The rotational distribution obtained from the photolysis of NO_2(80 mtorr) alone resulted in a complete thermal distribution of $T_{rot} = 560$ K extending to $N'' = 6$, which is plotted in Figure 3. By assuming a linear surprisal for the rotational distribution of OH($v''=0$, $N'' > 6$) produced from reaction 5, the micropopulations of OH($N'' \leq 6$ in $v''=0$) are corrected for the contribution of OH produced from direct photodissociation of HONO. The corrected micropopulations of OH($v''=0$) from reaction 5 are presented in Figure 2, where those from reaction 8 are also plotted as a dotted line. The upper limit of error in evaluating the vibrational population of OH in its ground state due to the surprisal correction is estimated to be no more than 30 %. The upper bounds of the errors are also presented in Figure 2. At this point, a possibility cannot be excluded that the thermal distribution ($T_{rot} = 750$ K) of OH below $N''=6$ in $v''=0$ observed in reaction 2. (Figure 2 in reference 6) which was interpreted as a bimodal distribution as mentioned in Introduction, might be due to the contribution of unwanted photolysis of HONO. This will be discussed in later section.

Electronic Distributions. Analysis of the spectra reveals that the ratio of the fine structure state micropopulations

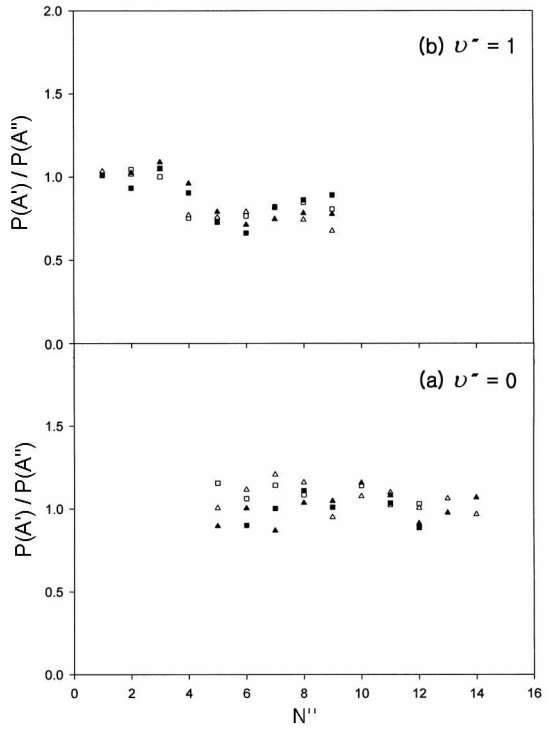

Figure 4. Dependence of Λ doublet population ratios $P(A')/P(A'')$ upon rotational state in (a) OH($X^2\Pi$, $v''=0$) and (b) OH($X^2\Pi$, $v''=1$). The ratios were obtained from the following transitions: P_{11}/Q_{11} (□), R_{11}/Q_{11}(_), P_{22}/Q_{22} (■), R_{22}/Q_{22} (▲). The ratios for the $N'' \leq 6$ states in $v''=0$ are not included because of the reason explained in the text.

summed over all the accessible rotational levels is about the same within the experimental errors for the two vibrational states. $P(^2\Pi_{3/2})/P(^2\Pi_{1/2}) = 1.06 \pm 0.1$ for OH($X^2\Pi$, $v''=0$), and 1.13 ± 0.1 for OH($X^2\Pi$, $v''=1$). Thus, there is no significant difference between the populations of the fine structure levels in the lowest vibrational state and a slight difference favoring the production of the lower level($^2\Pi_{3/2}$) in $v''=1$.

No specificity for production of either of the two Λ doublet states can be discerned from the micropopulations. The relative populations of OH produced in the Π(A') and Π(A") states, probed by the P/R and Q branches, respectively, are plotted in Figure 4; $P(A')/P(A'') = 1.07 \pm 0.1$ for OH($X^2\Pi$, $v''=0$), and 0.90 ± 0.1 for OH($X^2\Pi$, $v''=1$). The ratios for the $N'' \leq 6$ states in $v''=0$ are not included because of the uncertainty caused by the surprisal corrections described above. No preference for the Λ doublet states may be contrasted to the observation[21] of preferred Π(A') level population in the reaction of $O(^1D_2)$ with H_2. This reaction clearly proceeds *via* insertion of the excited oxygen atom into the H-H bond, with subsequent dissociation of the H-OH bond yielding preferential production of OH radicals with the half-filled π orbital oriented in their rotation plane and that of the triatomic collision complex. Indeed, failure to observe such preferential Λ doublet production following reaction 5 strongly suggests that OH formation results from direct attack of $O(^3P_J)$ upon the hydrogen atom by a direct abstraction mechanism. This would preclude preferential orientation of the π orbital in the collision complex. Table I contains a summary of the OH internal mode population distributions observed following the reaction of $O(^3P_J)$ with silane and trichlorosilane.

Vibrational Distributions. The abstraction mechanism is further supported by the population ratio of vibrational levels. Summation of the observed rotational distributions in $v''=0$ and 1 leads directly to an estimate of the relative populations of OH product formed in these two vibrational levels. $P(v''=1)/P(v''=0) = 4.0 \pm 0.6$. A primary source of error might come from the surprisal corrections of the low-J'' components as mentioned above. The other minor source of systematic error in this measurement arises from the need to correct the observed LIF emission signals for the wavelength dependent response of the filter-photomultiplier combination which could attenuate the fluorescence of the $A^2\Sigma(v'=1) \rightarrow X^2\Pi(v''=0)$ bands. The channeling of a large fraction, $\langle f_{vib} \rangle = 0.62$, of the available exoergicity into product vibration characterizes HL H′ reactions with early energy release (Table II). The product OH vibrational distribution resulting from reaction 2 is also highly inverted. $P(v''=1)/P(v''=0) = 3.4 \pm 0.4$, in good accord with the previously reported ratio of HF state populations deduced from an information theoretic treatment[22] of the reaction, $F(^2P_J) + SiH_4 \rightarrow HF + SiH_3$; $P(v''=1)/P(v''=0) = 3.1$. In general, such strongly inverted vibrational population ratios can be associated with the early release of reaction exoergicity along the reaction coordinate.

Reactions proceeding via an insertion/dissociation mechanism, for example, $O(^1D_2) + H_2 \rightarrow OH(X^2\Pi) + H$, can also result in the observation of a vibrational-state population inversion. The vibrational population inversion alone, however, does not support the insertion/dissociation mech-

anism. In the case of a relatively large substrate, the resulting collision complex, e.g., ROH* would be expected to be so long-lived and the available reaction exoergicity so broadly distributed as to preclude vibrational excitation of the diatomic product following dissociation of that complex. This intuitive view supports the observation that no vibrationally excited OH is formed following the reaction of $O(^1D_2)$ with alkanes larger than ethane.[23] The $OH(X^2\Pi)$ produced from reaction 3 also showed a strong vibrational population inversion; $P(\upsilon''=0)$: $P(\upsilon''=1)$: $P(\upsilon''=2)$ = 0:9:1, which was studied by both a crossed beam method and a bulk flow method. The two methods provided very similar OH product state distributions with a strong vibrational population inversion and substantial rotational excitation extending to the limit of available energy. The dynamics of the reaction 3 were considered to be consistent with expectations for the kinematically constrained reaction; heavy + light-heavy → heavy-light + heavy.

Disposal of the total available energies into the internal modes of OH product from the reactions 2 and 5 are listed in Table II. Since the first excited vibrational level of OH lies *ca.* 3,570 cm^{-1} above the zero-point level, one can easily find that the exothermicity ($-\Delta H^0$) alone is not quite sufficient to produce the vibrationally excited OH products for reaction 5. Observation of strong vibrational population inversion and substantially inverted rotational distributions in both vibrational states (Figure 2) clearly demonstrate that the collision energy (E_{coll}) of the O atom with $HSiCl_3$ is effectively converted to the excitation of internal modes of the diatomic.

While the total average available energies for both reactions 2 and 5 are essentially the same (*ca.* 4,600 cm^{-1}), the collision energies are different as much as about 30% as shown in Table II. Because the $HSiCl_3$ is heavier than SiH_4 by a factor of 4.2, more (*ca.* 330 cm^{-1}) of the excess collision energy is estimated to appear in the center-of-mass frame collision. Despite of the lower reaction exothermicity of reaction 5, the observation that a larger fraction of available energy is partitioned into the internal degrees of freedom compared to reaction 2 clearly demonstrates that the translational energies of the reactants are very efficiently coupled to the internal modes of the diatomic product, especially to the rotational mode (see Table II).

Rotational Distributions. The rotational distribution in Figure 2 shows that the most highly excited observed state extends to J'' = 15.5 ($E_{internal}$ = 4,341 cm^{-1}) at $\upsilon''=0$, and J'' = 9.5 ($E_{internal}$ = 5,157 cm^{-1}) at $\upsilon''=1$. These values can be compared with the 3,770 cm^{-1} ($-\Delta H^0 + 3kT$) nominally available to the reaction of thermalized reagents at 300 K. This observation ensures that the range of the excess kinetic energies carried by the O atom generated by the photolysis of NO_2 is quite broad,[13] and effectively couples into the diatomic's rotation.

A careful examination reveals that the rotational distributions of the OH products of reaction 5 are more inverted compared to those of reaction 2, especially in $\upsilon''=1$ state. The micropopulations of $OH(X^2\Pi, \upsilon''=1)$ in reaction 2 decrease monotonically (Figure 2 in reference 6) to give a thermal distribution with T_{rot}= 600 ± 20 K. Those in reaction 5, on the other hand, have negative temperature region at relatively low rotational levels (maximum at N'' = 5) and demonstrate a substantial excitation of rotational distribution. In comparison with the energetics of reaction 2, it can be concluded that the excess collision energy in reaction 5 is more efficiently channeled into the rotational excitation of the diatomic product as well as the vibrational excitation. The rotational micropopulation of $OH(X^2\Pi, \upsilon''=0)$ derived in each reaction shows a maximum at N'' = 8.

The thermal distribution of $OH(\upsilon''=0)$ at low rotational states ($N''\leq 6$) and the inverted distribution at higher states observed in reaction 2.(T_{rot} = 750 K)[6] was interpreted as a bimodal distribution, which led to a conclusion to support the existence of two different mechanisms for reaction 2. The thermal distribution of OH for all J'''s in $\upsilon''=1$ state and for low-J'' part in $\upsilon''=0$ state were attributed to a direct H atom abstraction by the O atoms, while the rotational inversion in $\upsilon''=0$ state led to a suggestion of a penta-valent bridged intermediate structure. From a dramatic difference between the $OH(\upsilon''=1)$ rotational distributions in reaction 2 and 5, and an experimental evidence of the formation of low-J'' components of $OH(\upsilon''=0)$ *via* reaction 8, it seems more reasonable to conclude that the $OH(X^2\Pi, \upsilon''=0,1)$ radicals produced in reaction 5 are formed through a direct abstraction mechanism; H + LH′ → HL + H′ reaction.

The overall shape of the observed rotational distributions derived from reaction 5 clearly inverts in a manner quite similar to product OH distributions arising from the reactions of electronically excited $O(^1D_2)$ with hydrogen-containing molecules except for the Λ doublet preferences which provide a crucial evidence for the reaction mechanisms, i.e., a simple abstraction *vs.* an insertion/dissociation. The $O(^3P_J)$ + $HSiCl_3$ system is contrasted with previously studied reactions of $O(^3P_J)$ with hydrocarbon molecules ($O(^3P_J)$ + RH), in which the OH product exhibits very little rotational excitation. This discrepancy in the degree of product rotational excitations between these two reaction systems can be attributed to the different angular dependence of the potential surfaces orthogonal to the reaction coordinate. The inverted rotational distribution of diatomic product in reaction 3 has been satisfactorily reproduced by K. G. McKendrick *et al.*[8] through QCT calculations on the $O(^3P_J)$ + HBr LEPS surface. The rotational population inversion of $OH(X^2\Pi, \upsilon''=1)$ in the reaction of O with H_2S has also been reported,[9] and led to the conclusion of efficient conversion of reagent kinetic energy into the OH product rotation.

Conclusion

The internal energy distributions of OH produced from the reaction, $O(^3P_J)$ + $HSiCl_3$ → $OH(X^2\Pi)$ + $SiCl_3$, has been measured utilizing the LIF method. The highly inverted vibrational distributions and no preference for the Λ doublet states can be interpreted in terms of a direct abstraction mechanism for a H + LH′ → HL + H′ reaction system. The substantial rotational excitation of the $OH(X^2\Pi, \upsilon''=0$ and 1) product is distinctly different from the extremely cold rotational distributions observed in previous reactions of $O(^3P_J)$ with larger hydrocarbons. The excitation of the internal modes of the

diatomic product in the title reaction is rather similar to that observed in the reactions, $O(^3P_J)$ + HBr, and $O(^3P_J)$ + H_2S. The degree of rotational excitation of the diatomic product can be rationalized in terms of different angular dependences of the model potential surfaces along the reaction coordinate. The excess kinetic energy of the title reaction seems to contribute to the efficient mapping of translation into rotation of diatomic product, presumably by facilitating the angular excursions of the O atom to climb up the potential surface perpendicular to the reaction coordinate.

Acknowledgments. This work was financially supported by the Korea Science and Engineering Foundation (Grant No. R01-2003-000-10886-0), and partly by the research program 2005 of Kookmin University in Korea.

References

1. (a) Zhang, Q.; Gu, Y.; Wang, S. *J. Chem. Phys.* **2003**, *118*, 633. (b) Zhang, Q. Z.; Wang, C. S.; Wang, S. K.; Gu, Y. S. *Chinese Chemical Letters* **2002**, *13*, 662. (c) Huynh, L. K.; Zhang, S.; Truong, T. N. *Combustion and Flame* **2008**, *152*, 177. (d) Nam, M. J.; Youn, S. E.; Li., L.; Choi, J. H. *J. Chem. Phys.* **2005**, *123*, 211105. (e) Balucani, N.; Stranges, D.; Casavecchia, P.; Volpi, G. G. *J. Chem. Phys.* **2004**, *120*, 9571. (f) Garton, D. J.; Minton, T. K. *J. Phys. Chem. A* **2003**, *107*, 4583. (g) Troya, D.; Garcia-Molina, E. *J. Phys. Chem. A* **2005**, *109*, 3015. (h) Capozza, G.; Segoloni, E.; Leonori, F.; Volpi, G. G.; Casavecchia, P. *J. Chem. Phys.* **2004**, *120*, 4557.
2. (a) Rand, R. J. *J. Vac. Sci. Technol.* **1979**, *16*, 420. (b) Boyer, P. K.; Roche, G. A.; Ritchie, W. H.; Collins, G. J. *Appl. Phys. Lett.* ***1982***, *40*, 716. (c) Chen, J. Y.; Henderson, R. C.; Hall, J. T.; Peters, J. W. *J. Electrochem. Soc.* ***1984***, *131*, 2146.
3. (a) Herron, J. T.; Huie, R. E. *J. Phys. Chem. Ref. Data* **1974**, *2*, 467. (b) Huie, R. E.; Herron, J. T. *Prog. React. Kinet.* **1975**, *8*, 1.
4. (a) Andresen, P.; Luntz, A. C. *J. Chem. Phys.* **1980**, *72*, 5842. (b) Luntz, A. C.; Andresen, P. *J. Chem. Phys.* **1980**, *72*, 5851. (c) Kleinermanns, K.; Luntz, A. C. *J. Chem. Phys.* **1982**, *77*, 3533. (d) Kleinermanns, K.; Luntz, A. C. *J. Chem. Phys.* **1982**, *77*, 3774. (e) Kleinermanns, K.; Luntz, A. C. *J. Chem. Phys.* **1982**, *77*, 3537. (f) Dutton, N. J.; Fletcher, I. W.; Whitehead, J. C. *Mol. Phys.* **1984**, *52*, 475. (g) Barry, N. J.; Fletcher, I. W.; Whitehead, J. C. *J. Phys. Chem.* **1986**, *90*, 491. (h) Dutton, N. J.; Fletcher, I. W.; Whitehead, J. C. *J. Phys. Chem.* **1985**, *89*, 569.
5. Duewer, W. H.; Setser, D. W. *J. Chem. Phys.* **1973**, *58*, 2310.
6. Park, C. R.; White, G. D.; Wiesenfeld, J. R. *J. Phys. Chem.* **1988**, *92*, 152.
7. (a) Luntz, A. C.; Schinke, R.; Lester, Jr., W. A.; Gunthard, Hs. H. *J. Chem. Phys.* **1979**, *70*, 5908. (b) Saunders, N. D.; Butler, J. E.; McDonald, J. R. *J. Chem. Phys.* **1980**, *73*, 5381. (c) Smith, G. K.; Butler, J. E. *J. Chem. Phys.* **1980**, *73*, 2243. (d) Luntz, A. C. *J. Chem. Phys.* **1980**, *73*, 1143. (e) Butler, J. E.; Jursich, G. M.; Watson, I. A.; Wiesenfeld, J. R. *J. Chem. Phys.* **1986**, *84*, 5365. (f) Aker, P. M.; Sloan, J. J. *J. Chem. Phys.* **1986**, *85*, 1412.
8. McKendrick, K. G.; Rakestraw, D. J.; Zare, R. N. *J. Phys. Chem.* **1988**, *92*, 5530.
9. Costen, M. L.; Hancock, G.; Ritchie, G. A. D. *J. Phys. Chem. A* **1999**, *103*, 10644.
10. Park, C. R.; Wiesenfeld, J. R. *J. Phys. Chem.* **1989**, *93*, 1365.
11. (a) Magrini, K. A.; Gebhard, S. C.; Koel, B. E.; Falconer, J. L. *Surface Science* **1991**, *248*, 93. (b) Krasnova, T. L.; Abramova, E. S.; Alekseev, N. V.; Chernyshev, E. A. *Russian Chemical Bulletin* **1999**, *48*, 1960.
12. Ding, L.; Marshell, P. *J. Am. Chem. Soc.* **1992**, *114*, 5754.
13. Busch, G. E.; Wilson, K. R. *J. Chem. Phys.* **1972**, *56*, 3626.
14. Luque, J.; Crosley, D. R. *LIFBASE: Database and Spectral Simulation Program*, Version 1.5; SRI International Report MP 99-009, 1999.
15. Doncaster, A. M.; Walsh, R. *J. Chem. Soc., Faraday Trans. I* **1979**, *75*, 1126.
16. Doncaster, A. M.; Walsh, R. *Int. J. Chem. Kinet.* **1981**, *13*, 503.
17. Walsh, R. *Acc. Chem. Res.* **1981**, *14*, 246.
18. Moor, E. A.; Richards, W. G. *Phys. Scr.* **1971**, *3*, 223.
19. Whitehead, J. C. *Gen. Discuss., Faraday Discuss. Chem. Soc.* **1991**, *91*, 151.
20. Bernstein, R. B. *Chemical Dynamics via Molecular Beam and Laser Techniques*; Oxford Science: 1982; p 196.
21. Cleveland, C. B.; Jursich, G. M.; Trolier, M.; Wiesenfeld, J. R. *J. Chem. Phys.* **1987**, *86*, 3253.
22. Bogan, D. J.; Setser, D. W. *J. Chem. Phys.* **1976**, *64*, 586.
23. Park, C. R.; Wiesenfeld, J. R. *J. Chem. Phys.* **1991**, *95*, 8166.